Egypt. J. Chem. **Vol. 67**, No. 12 pp. 451 - 464 (2024)

Egyptian Journal of Chemistry

http://ejchem.journals.ekb.eg/

Outstanding Styrene-Butadiene Rubber Composites Enhanced by Surface-Modified Fillers

Salwa H. El-Sabbagh[a]*, Mohamed M. Selim[b], Gamal Abd El-Naeem[c], Doaa Samir Mahmoud[a], Amir A. Abdelsalam[d]

[a]*Polymers and Pigments Department, National Research Centre, Cairo 12311, Egypt*

[b]*Physical Chemistry Department, National Research Centre, Cairo 12311, Egypt*

[c]*Polymer Materials Research Department, City for Scientific Research and Technology Applications, New Borg El-Arab City 21934, Alexandria, Egypt*

[d]*Mechanical Engineering Department, Benha Faculty of Engineering, Benha University, Benha 13511, Egypt*

Abstract

The research findings on the mechanical properties of styrene-butadiene rubber (SBR) composites, particularly the impact of aging temperatures, have practical implications. To evaluate this effect, the study used a thermal aging test at various temperatures. The work developed SBR filled with several fillers, including kaolin, metakaolinite, zeolite Na-A, Al_2O_3, and synthetic zeolite Na-A/Al_2O_3 nanoparticles. A hybridization of SBR-filled synthetic zeolite Na-A/ Al_2O_3 composite was also created. The rubber mixer of two-roll mill was used to compound the material, with a filler loading of 1-5 phr. The mechanical properties of the elastomeric composites were determined before and after thermal-oxidative aging using an air-circulating oven. The respective composites were tested at varied aging times. A thermogravimetric analyzer (TGA) was used to measure thermal stability. The surface morphology of broken rubber composites was examined using a scanning electron microscope (SEM). Here, a comparative there is a comparative study of the Cross-link density estimations of cured SBR utilizing swelling and Mooney-Rivlin methods. The data from different comparison approaches yielded similar results, giving us considerable confidence in our research. Aging studies revealed that zeolite Na-A/Al_2O_3/SBR composite showed superior anti-aging properties in comparison to the other composite. The most effective, straightforward, and environmentally friendly technique for determining the Cross-link density of cured rubber was found to be the Mooney-Rivlin equation. Our research methods are more trustworthy because this process is based on mathematics and doesn't involve any hazardous chemicals or solvents. This study recommends using zeolite Na-A/Al_2O_3 as a cost-saving filler in SBR composites, which has practical implications for the industry.

Keywords: Thermal Aging; Thermogravimetric analysis; Treated filler; SBR composites; Tensile Properties.

1. Introduction

Rubber is now widely used in automobiles, food packaging, medicine, and aerospace [1]. Some examples of industrial elastomers utilized in the industries as mentioned above include natural rubber (NR), butadiene rubber (BR), styrene-butadiene rubber (SBR), silicon rubber (SR), and nitrile rubber (NBR). Tire manufacturing is one of the most well-known applications for rubber in the automotive industry, and it is critical to human well-being. Tires are complex items composed of numerous rubbery portions, such as crowns, gum, beads, tread, inner layers, and side walls, typically of SBR, BR, NR, etc. Rubber accounts for around 40-50% of a tire [2,3]. SBR and BR rubbers usually account for 60-70 percent of a tire's rubbery components [4]. This is due to its advantageous qualities, including hardness and chemical and water resistance. SBR tires are commonly used in construction machines and underground mining because of their rigidity and minimal hysteresis, resulting in superior puncture and cut resistance [5–7].

*Corresponding author e-mail: salwa_elsabbagh@yahoo.com.;(Salwa H. El-Sabbagh).
EJCHEM use only: Received date 24 September 2024; revised date 16 October 2024; accepted date 21 October 2024
DOI: 10.21608/ejchem.2024.323463.10503

Rubber aging is a protracted and ongoing process. The primary technique used in rubber-aging research is called the "accelerated rubber-aging test" in a controlled which is done in a controlled environment to examine how rubber properties change as it ages. The closest aging technique to real natural aging is believed to be oven-The closest aging technique to real natural aging is believed to be oven-accelerated aging. Rubber is exposed to various environmental conditions during use and storage, which affects the rubber product's service life and degrades its performance. Rubber aging is complex since different usage settings have varying needs for rubber features.

Accelerated aging at high temperatures is one of the primary methods used in testing to imitate a rubber-aging environment. The most frequent strategy for improving the thermal characteristics of rubber is to add antioxidants or inorganic fillers [8,9]. Indeed, rubber degradation is quite sluggish in a real-world working environment; therefore, obtaining rubber with degradation behaviors takes a long time. Accelerated aging tests are often used to evaluate the degradation of rubbers in a relatively short time [10]. Inorganic fillers were primarily utilized due to their lower cost and ability to achieve the white colour of rubber products.

The presence of inorganic nanoparticles in the composite media improves the thermal diffusivity of the tire compound, allowing for optimal heat transfer within the tire. Furthermore, heat transfer avoids tire explosion while driving by increasing the internal air temperature of the tire, especially in hot weather [1,11]. Accelerated aging tests are commonly performed to measure vulcanizate oxidation resistance. Most research on elastomer aging has focused on changes in the elastomer's chemical composition caused by prolonged exposure to heat, oxygen, ozone, and other conditions. Thermal aging can cause main-chain scission, Cross-link creation, and Cross-link breakage, resulting in severe changes in the mechanical characteristics of elastomers [12–14]. The most crucial issue with using high-temperature rubber is oxidative deterioration. Thermal aging clarifies the most desired features required in the rubber sector, such as tension, compression, and hardness. Hence, various investigators have studied the effect of fillers on these properties.

Shaojian He et al. [8] investigated the effects of carbon black filler loading on SBR's microstructure and mechanical properties. The effect of thermal aging in the air over time on the mechanical characteristics of SBR composites was also examined. At 100% strain, the SBR/CB composite exhibited the highest aging coefficient and the slowest change in tensile strength and stress. A. Mostafa et al. [15] built on the work of Shaojian He et al. [8] by investigating the influence of CB loading on the ability of filled SBR to tolerate the effect of thermal aging at various aging temperatures on the tension, compression, and hardness properties of SBR elastomer. Many studies have extensively researched the thermal aging behavior of filled rubber. However, the effect of hybrid filler loading on the aging resistance of SBR compounds is rarely addressed [15–17]. When cross-linking occurs in rubber-like flexible materials, the elastic modulus increases noticeably, the hardness increases, and final elongation and permanent set decrease most of the time. The physical characteristics of a vulcanizate are significantly influenced by its cross-link density [18].

The main objective of this research is to investigate how hybrid and different fillers affect the ability of filled elastomers to endure thermal aging at various temperatures. The study also aims to compare SBR composites' Cross-link densities as measured by: Tensile strength results, the Mooney–Rivlin Method, and the Flory- Rehner equation. Fillers ranging from 1 to 5 phr were added to the SBR compound. The variation of compound and vulcanizate characteristics with filler content was examined.

2. Experimental

2.1. Materials

The composites were made of SBR, fillers (kaolin, metakaolinite, synthetic zeolite Na-A, Al_2O_3 nanoparticles, and hybrid filler synthetic zeolite Na-A/Al_2O_3), cure activators (stearic acid and zinc oxide (ZnO)), CBS was used as an accelerator; TMQ was used as an antioxidant. Egyptian Kaolin was supplied from El-Nile Co., Egypt. Ball milling was used to prepare micron-sized Al_2O_3 powders (120-320 nm). The silane 3-aminopropyltriethoxysilane (APTES) supplied by Sigma-Aldrich Company was used as received. Other standard rubber compounding ingredients, such as process oil and sulfur, were used at commercial grades. Synthesis of metakaolinite and zeolite Na-A from Kaolinite was revisited, and the method of surface treatment of filler was described in our previous article [19].

2.2. Preparation of rubber composites

The samples tested in this investigation consisted of SBR compounded with different amounts of fillers of

fillers, as shown in Table 1. Ingredients of the rubber compounds were mixed on a laboratory two-roll mill with an outer diameter of 470 mm, 300 mm length, the speed of slow roll being 24 rpm, and the gear ratio of 1.4. Then, stearic acid and ZnO were added. The investigated fillers were then introduced and mixed for sufficient time to disseminate the filler into the SBR rubber. The mixing procedure was resumed after adding the CBS, TMQ, and sulfur to the SBR rubber. Compression molding was used to vulcanize each type of rubber compound using a hot hydraulic press at 162 ± 1 °C and a pressure of about 4 MPa.

Table 1: Formulations of treated fillers/SBR compounds (phr)

Sample No. / Materials	Quantities (phr)					
	S1	S2	S3	S4	S5	S6
SBR	100	100	100	100	100	100
Stearic acid	2	2	2	2	2	2
ZnO	5	5	5	5	5	5
CBS	1	1	1	1	1	1
TMQ	1	1	1	1	1	1
Sulfur	2	2	2	2	2	2
Treated fillers	0	1	2	3	4	5
Processing Oil	1	1	1	1	1	1

Notes: phr (part per hundred of rubber); SBR1502, styrene-butadiene rubber with 23.5 wt% of styrene content; N-cyclohexyl-2-benzothiazole sulfenamide (CBS); polymerized 2,2,4-trimethyl-1,2-dihydroquinoline (TMQ); treated filler (Al_2O_3, zeolite Na-A, zeolite Na-A/Al_2O_3, kaolin and metakaolinite)

2.3. Tests performed on rubber composites

2.3.1. Aging Characteristics of fillers/SBR composites

The tensile properties of the cured filler/SBR vulcanizates were determined using a Zwick 1425 universal testing machine according to ASTM D 412-16 [20]. The tensile characteristics of composites were calculated using an average of five distinct samples for each formulation. The tensile test was performed at ambient temperature and 500 mm/min speed to determine the tensile parameters of the cured samples, including tensile strength, elongation at break, and tensile modulus.

The filler-reinforced composites based on SBR rubber were thermally aged for 2, 4, 6, and 7 days in an air circulation oven at 90 ^{0}C, following ASTM D573 - 04 [21]. The specimens were cooled and maintained at room temperature for at least 24 hours until the tensile characteristics of the old specimens matched those of the non-aged specimens. The maintained percentage values for tensile strength and elongation at break were calculated. Tensile characteristics (tensile strength and elongation at break) were tested before and following aging tests.

2.3.2. Swelling Properties

Rubber vulcanizate equilibrium swelling studies were conducted in toluene at room temperature (25°C) according to ASTM D471-12a [22]. Approximately 0.5 g of each cured specimen was immersed in toluene for 48 hours to achieve equilibrium swelling. The swelled samples were weighed and then oven-dried to a consistent weight. After drying, the rubber sample's weight was determined to be free of dissolved materials. The swelling percentage (Q%) of the rubber samples was assessed using Eq. 1:

$$Q\,\% = \frac{W_2 - W_1}{W_1} \times 100 \qquad \text{Eq. 1}$$

Where, W_2 and W_1 represent the swollen weight and dried weight of the samples, respectively.
The rubber–filler interaction was evaluated using the Lorenz and Park Eq. 2 [23]:

$$\frac{Q_{filler}}{Q_{gum}} = ae^{-z} + b \qquad \text{Eq. 2}$$

Q_{filler} is the filler's swelling value, and Q_{gum} is the swelling value of the gum. Z is the filler weight ratio in the vulcanizate, whereas a and b are constants. The

swelling ratio (Q_{filler}/Q_{gum}) is lower when the filler and rubber matrix interact correctly.

The degree of reinforcement was measured by the Cunneen and Russell [24]equation as follows Eq. 3:

$$\frac{v_{ro}}{v_{rf}} = ae^{-z} + b \qquad \text{Eq. 3}$$

Where V_{r0} is the volume fraction of the gum rubber vulcanizates, and V_{rf} is the volume fraction of the rubber network in the swollen phase; z, a, and b are the same as defined earlier.

2.3.3. Mooney-Rivlin Method for Analyzing Cross-Link Densities Based on Tensile Strength Results

The Mooney-Rivlin method can be used to calculate cross-link density (νe) using tensile strength test data [25]. Eq. 4was utilized to compute the linear regression graphs and network parameters [26].

$$\frac{\sigma}{2(\lambda - \lambda^{-2})} = C_1 + \frac{C_2}{\lambda} \qquad \text{Eq. 4}$$

Where σ is the true stress; λ is the extension rate; C_1 is the contribution of Cross-linking units; C_2 is the Mooney–Rivlin elastic constant, representing the contribution of fixed entanglements. The material constant C_1 can be used to calculate cross-link densities using Eq. 5 [27].

$$v_e = \frac{C_1}{RT} \qquad \text{Eq. 5}$$

Where η is the cross-linking density (mol cm^{-3}); R is the universal gas constant (8.314 $J.mole^{-1}.K^{-1}$); and T is the absolute temperature (K).

2.3.4. Thermogravimetric analyzer (TGA)

The thermal degradation properties of samples were measured using a thermogravimetric analyzer (TA Instruments, TGA Q5000, USA). The mass loss during heating from ambient temperature to 600 °C at a rate of 10 °C/min was measured. Approximately 5 mg of test samples were evaluated in a nitrogen environment with a 40 ml/min gas flow rate.

2.3.5. Scanning Electron Microscopy (SEM)

SEM micrographs of the tensile fracture surface of rubber vulcanizates were collected to examine the influence of filler dispersion in the rubber matrix. The microstructure and morphological properties of the samples were analyzed with a JEOL JSM 6360LA, Tokyo, Japan.

3. Results and Discussions

3.1. Aging Characteristics of filler/SBR composites

Thermal stability is defined as the exact temperature and duration at which a material can be used without suffering significant property loss [8,28]. Several ways have been devised to track the aging of rubbers. Tensile strength and elongation at break testing are frequently recognized as the most immediate and valuable indications of the remaining mechanical qualities. Cross-linking operations were carried out in an air-circulating oven at 90 ^{0}C for 2, 4, 6, and 7 days to study the effect of thermal aging on the mechanical properties of rubber composite materials. Fig. 1 and Fig. 2 display the tensile strength and strain at rupture after age, respectively. The results demonstrate that aged fillers/ SBR composites have lower tensile strength and elongation at break. However, the aged unfilled SBR's tensile strength and strain at rupture improved as compared to their mechanical attributes before aging. The effect of air aging on the mechanical characteristics of a fillers/ SBR composite with the same filler content (3phr) was investigated. After 7 days of aging, the zeolite Na-A/Al_2O_3/ SBR composite tensile strength was 3.11 MPa, significantly greater than that of the zeolite Na-A/SBR and Al_2O_3/SBR, respectively.

Zeolite Na-A/Al_2O_3/SBR composite had superior anti-aging properties than Zeolite Na-A/SBR and Al_2O_3/SBR composite. The good anti-aging characteristics of filler/rubber composites have been attributed to the fine dispersion of filler in the rubber matrix and the strong interfacial adhesion between filler and rubber chains [8]. Tensile strength decreases with prolonged aging time, primarily due to inhomogeneous Cross-linking during the thermal aging process [8,29]. As indicated in Fig. 2, decreasing elongation at break was seen with increasing aging time. Such occurrences can be explained as follows: during thermal aging in air, SBR macromolecular chains Cross-link. Higher Cross-linking degrees result in harsher limitation of chain extension and a more significant drop in chain length between Cross-linking locations, making SBR stiffer and more brittle [8,30,31].

Plotting the property aging coefficients of SBR composites against fillers/SBR composites was done in order to measure the impact of thermal aging on the different mechanical qualities that were investigated. The results are displayed in Fig. 3. The graph indicates that, as the filler % grows, the value of the property aging coefficients gradually declines. As was previously mentioned, fillers and SBR composites with more unusual filler compositions age less well. Moreover, as seen in Fig. 3, the conserved values of the assessed qualities first increased, presumably as a result of improved cross-linking with aging that slowed down the early stages of

degradation. However, as aging time increased due to deterioration, these values decreased [32]. The conserved stress values and strain at rupture are shown to decrease with age, according to these statistics. On the other hand, the aging coefficients of SBR composites are displayed in Figure 3. In general, as aging time increases, the aging coefficient of all SBR composites decreases, as Fig. 3 shows. Greater anti-aging efficacy is indicated by an increased aging coefficient (AC) [33]. Of all the composite samples, Figure 3 demonstrates that the AC of 1 phr of Al_2O_3 is the highest. Since Al_2O_3/ silane 3-aminopropyltriethoxysilane (APTES) seem to promote firm rubber contact, the aging coefficient indicates that samples loaded with Al_2O_3 have a better thermal resistance. This increase in thermal aging could be explained by the presence of silanol groups, which appear to facilitate firm rubber contact.

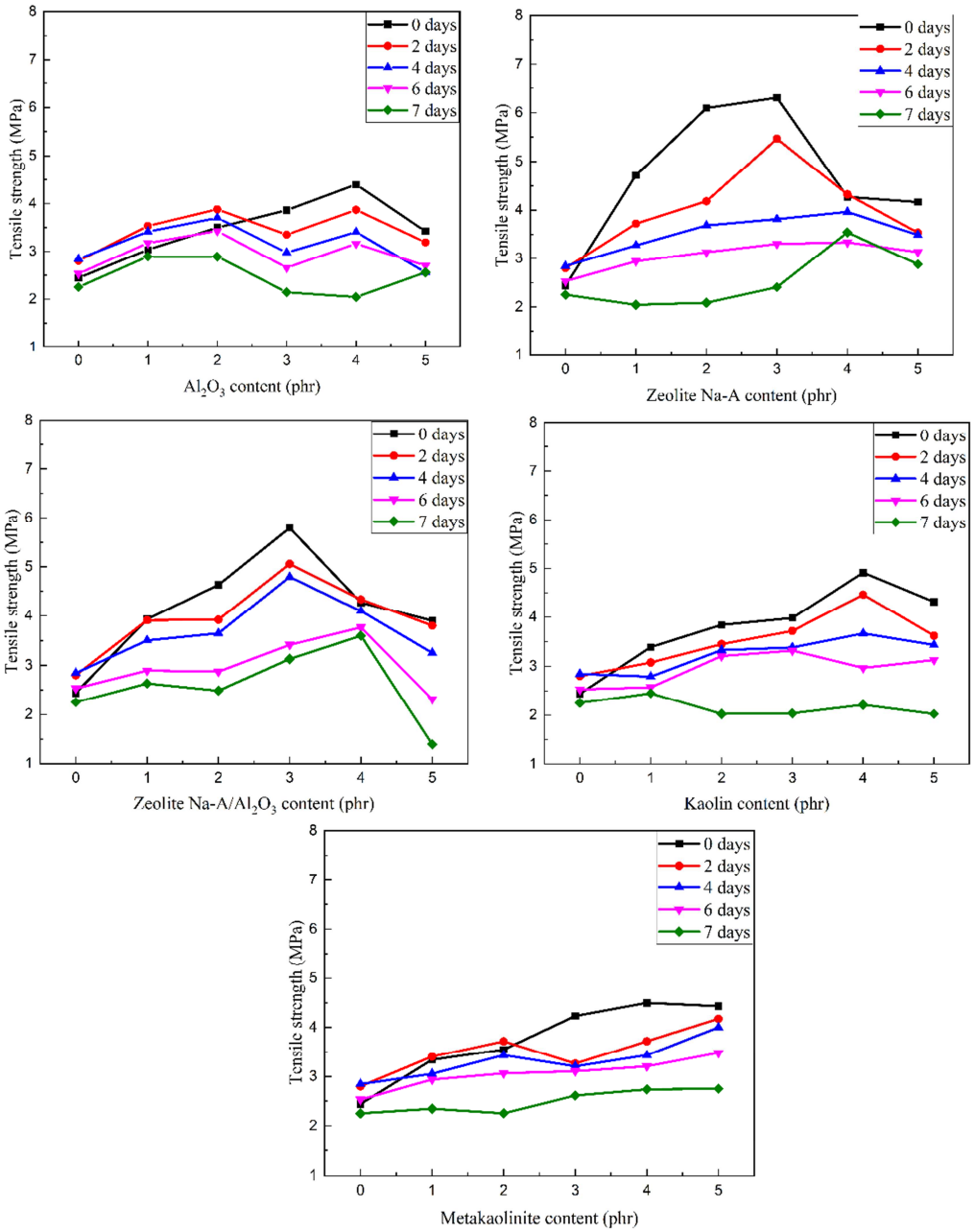

Figure 1: The tensile strength of SBR composites loaded various fillers both before and after aging.

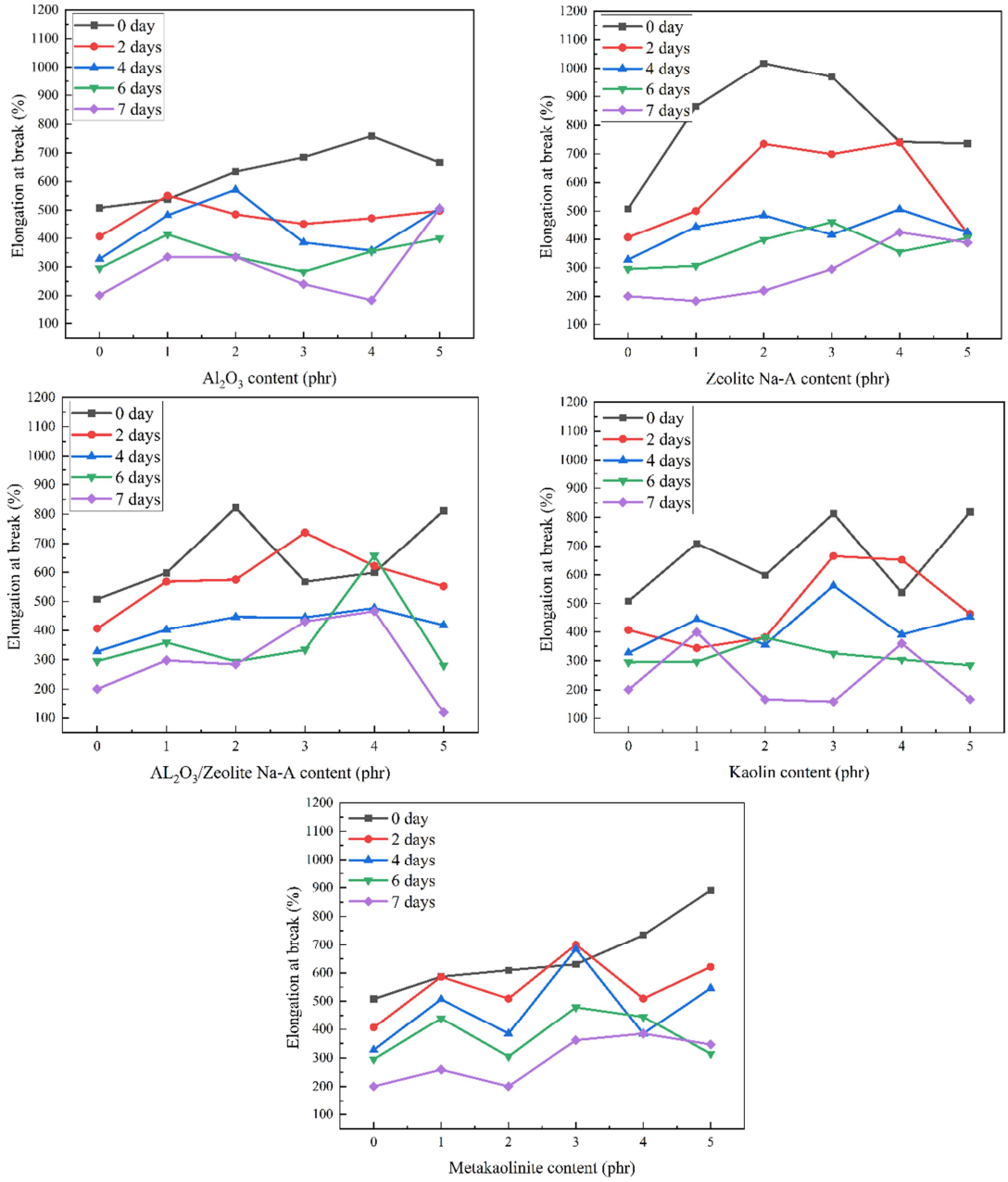

Figure 2: The elongation at break (%) for SBR loaded different filler both before and after aging.

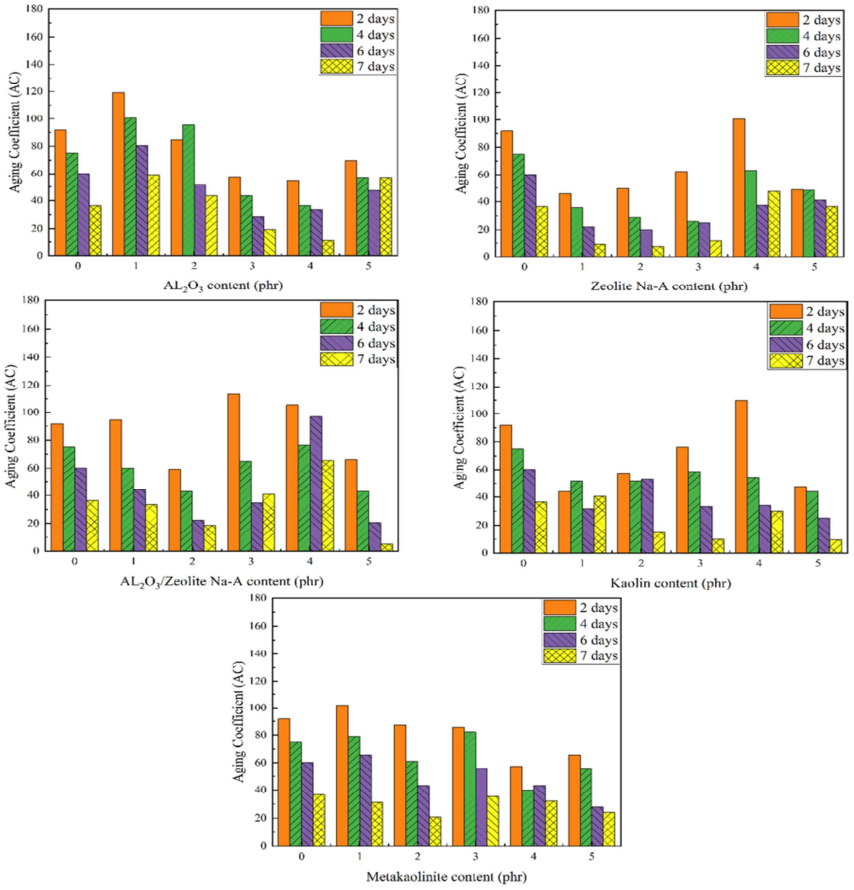

Figure 3: Dependence of the aging coefficient on the aging time for SBR loaded with different filler concentrations.

3.2. Swelling analysis

Polymeric materials can swell when exposed to diverse solvents during service applications, posing intellectual and technological challenges. Equilibrium swelling is extensively used to assess the average molecular weight, M_C, of Cross-links, which is directly proportional to Cross-link density [34]. Rubber-filler interaction was investigated better to understand the reinforcing process in filler rubber composites. Rubber-filler interactions were examined by calculating the volume fraction (V_{rf}) of rubber in swollen composites as a measure of Cross-link density. Fig. 4(a) compares the volume fraction of the rubber network in the swelling phase (V_{rf}) to the filler content in the filler rubber composites. The Fig. shows that when filler loading increases, the composite's solvent absorption diminishes, leading to a rise in V_{rf}. The high amount of contact between rubber and filler in the presence of metakaolinite results in developing a chemical link between SBR's pendent ethoxy groups and metakaolinite's hydroxyl functional groups, increasing the value of V_{rf}.
Furthermore, Fig. 4 (b) demonstrates that the degree of swelling in filler rubber composites reduces as the filler quantity increases. Lower levels of edema with filler ingestion imply a stronger rubber-filler interaction. Fig. 4 (c) shows a straight line with a positive slope when plotting V_{r0}/V_{rf} versus e^{-z} using the Cunneen and Russell equation. This indicates the filler's ability to reinforce. The high value of a and the low value of b imply rubber-filler attachment, while V_{r0}/V_{rf} represents reinforcement. Thus, the Cunneen Russel plot confirms the filler's ability to reinforce SBR composites. Furthermore, as the filler content increases, the Cross-link density of the filler rubber composites increases as more Cross-link bonds form in the vicinity of the fillers, increasing the filler-rubber interaction.

Table 2: Slope parameters for Cunneen and Russel equation

Composites	a (slope)	b (intercept)
AL_2O_3/SBR	1.733	− 0.761
Zeolite Na-A/SBR	2.698	−1.628
AL_2O_3/Zeolite Na-A/SBR	3.589	− 2.585
Kaolin/SBR	2.597	− 1.704
Metakaolinite/SBR	3.923	− 2.947

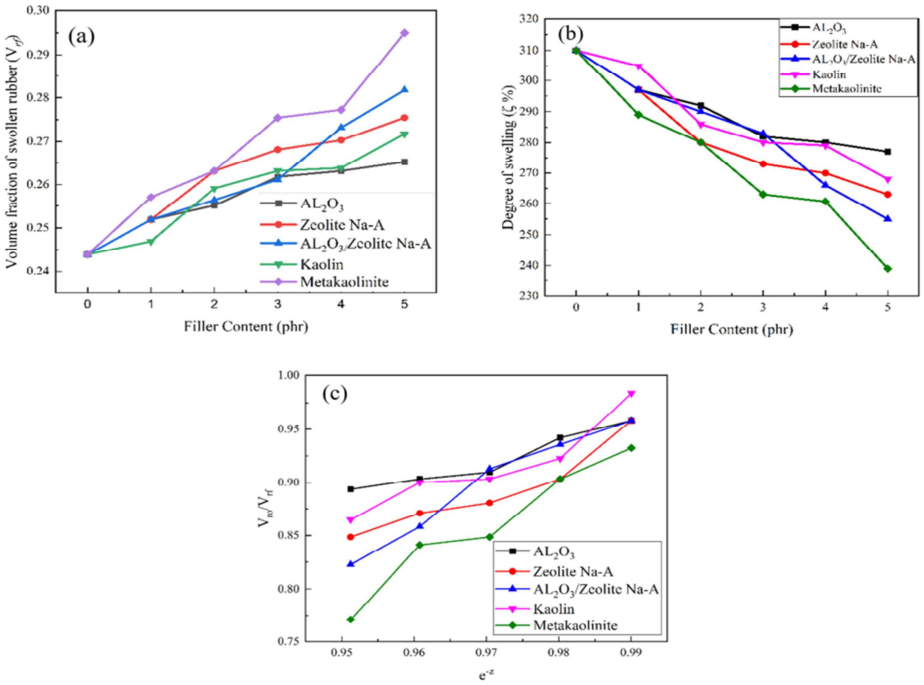

Figure 4: Effect of filler content on (a) the content volume fraction (V_{rf}), (b) the degree of swelling and (c) The change in V_{ro}/V_{rf} with e^{-Z} for SBR composites

3.3. Cross-link densities of fillers/SBR composites obtained using the Mooney–Rivlin method

C_1, the linear coefficient of the equation, describes the bonds created in the composites and is directly connected to the density of Cross-links. It has been observed that increasing fillers is associated with increasing C_1 and, as a result, increasing the density of cross-links. Furthermore, the value C_2, which reflects the slope coefficient and is connected to the polymer chain's intermolecular forces, increases. These results reveal the intensive interaction between the filler and the matrix, suggesting the reinforcement supplied by the filler and the cross-links [35,36].

Table 3: The value of constant C_1 and C_2 for Al_2O_3/SBR composites

Composites	C1 (MPa)	C2 (MPa)
S1	0.126	0.284
S2	0.184	0.210
S3	0.197	0.236
S4	0.203	0.284
S5	0.222	0.189
S6	0.190	0.255

Table 4: The value of constant C1 and C2 for zeolite Na-A /SBR composites

Composites	C_1 (MPa)	C_2 (MPa)
S1	0.126	0.284
S2	0.216	0.168
S3	0.249	0.184
S4	0.223	0.272
S5	0.228	0.124
S6	0.229	0.223

Table 5: The value of constant C_1 and C_2 for synthetic zeolite Na-A/Al_2O_3 /SBR composites

Composites	C1 (MPa)	C2 (MPa)
S1	0.126	0.284
S2	0.248	0.171
S3	0.222	0.215
S4	0.297	0.156
S5	0.264	0.183
S6	0.177	0.277

Table 6: The value of constant C_1 and C_2 for Kaoline/SBR composites

Composites	C_1 (MPa)	C_2 (MPa)
S1	0.126	0.284
S2	0.237	0.189
S3	0.252	0.204
S4	0.190	0.259
S5	0.353	0.228
S6	0.190	0.293

Table 7: The value of constant C_1 and C_2 for MetaKaoline/SBR composites

Composites	C_1 (MPa)	C_2 (MPa)
S1	0.126	0.284
S2	0.208	0.216
S3	0.207	0.179
S4	0.259	0.271
S5	0.229	0.196
S6	0.185	0.218

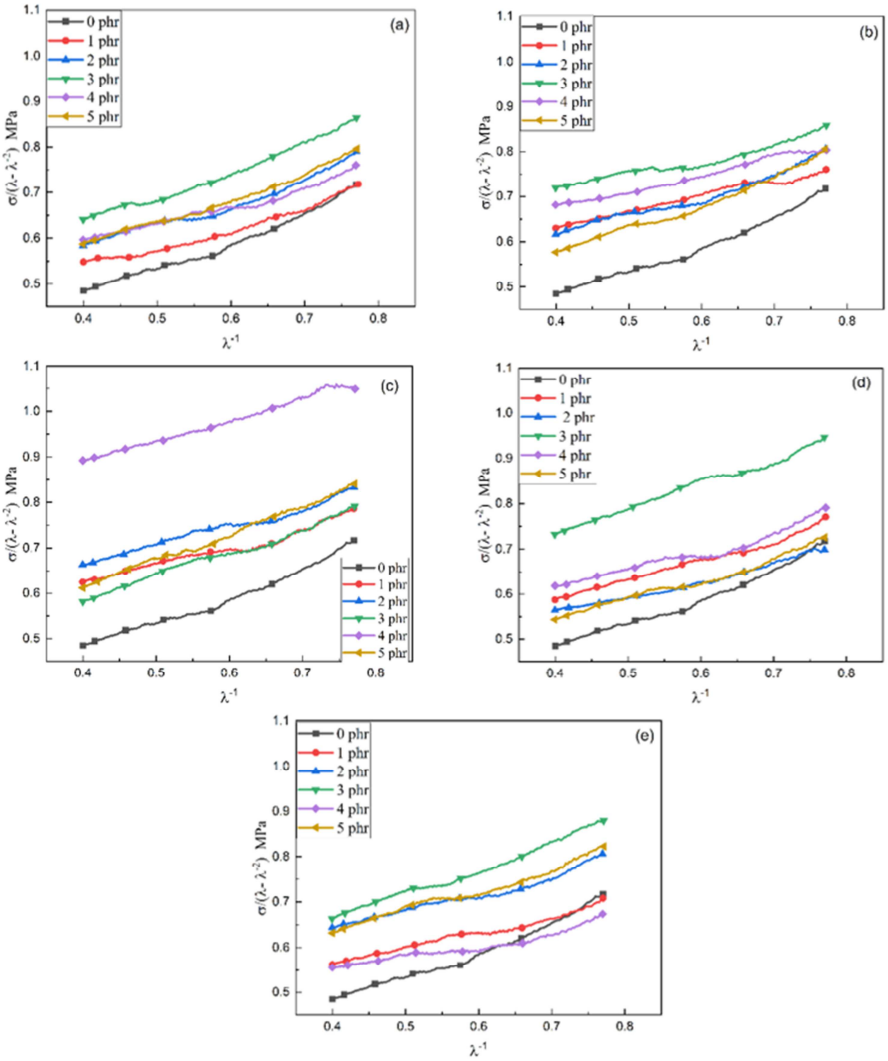

Figure 5: The Mooney-Rivlin plots for SBR composites filled with (a) Al_2O_3, (b) Zeolite Na-A, (c) (synthetic zeolite Na-A/Al_2O_3), (d) Kaolin, and (e) Metakaolinite.

Table 8 and Table 9 demonstrate the Cross-link densities of filler/SBR composites created using the two approaches. The Cross-link densities produced from the two distinct approaches are quite different, with the value obtained from the Mooney-Rilvin equation being significantly lower than that obtained from the Flory-Rehner equation. The gap in the results between the two methodologies discovered in this investigation was suggested to be driven by two possible explanations, which are [27]:

Mode of deformation: The deviance of the results is determined by the amplitude of the Cross-link fluctuations, which influences how loosely the Cross-links are embedded in the network structure. The stress-strain method (Mooney-Rilvin) caused the polymer chains to fully swell and stretch out, whereas the Flory-Rehner method did not. Errors in Flory-Rehner equation calculations: Because all of the parameters (X, *f*, and V_r) utilized were derived using different independent methods, an error in the calculations would occur.

Where χ is the Flory-Huggins interaction parameter for toluene and rubber, *f* is the filler ratio and V_r is the volume fraction of swollen rubber.

Table 8: Cross-link density (mol/m^3) of SBR composites from the Mooney-Rivlin Method

Composites	Al_2O_3	Zeolite	Synthetic zeolite Na-A/Al_2O_3	Kaoline	MetaKaoline
S1	50.872	50.872	50.872	50.872	50.872
S2	74.349	87.089	100.019	95.759	84.056
S3	79.485	100.300	89.559	101.529	83.745
S4	81.941	90.197	119.962	76.500	104.669
S5	89.418	91.904	106.588	142.648	92.498
S6	76.860	92.512	71.273	76.753	74.817

Table 9: Cross-link density (mol/m^3) of SBR composites from the Equilibrium swelling

Composites	Al_2O_3	Zeolite	Synthetic zeolite Na-A/Al_2O_3	Kaoline	MetaKaoline
S1	73.931	73.931	73.931	73.931	73.931
S2	79.619	78.051	85.926	75.375	83.979
S3	87.227	87.716	82.604	88.220	87.856
S4	90.377	99.368	79.998	85.803	99.979
S5	87.093	93.316	97.034	95.874	99.320
S6	81.925	91.293	105.425	89.346	81.033

3.4. Thermogravimetric analysis (TGA)

The thermal stability of composites was assessed using TGA. The starting decomposition temperature (Ti) is followed by T25, T50, and T75, representing weight losses of 25, 50, and 75 percent, respectively (Table 10).

According to Table 10, weight loss temperatures for all fillers except metakaolinite/SBR composites are higher than those for pure SBR rubber, which could be attributed to a maximized interaction between the filler particle and the SBR rubber due to the availability of a larger surface area of the particle in the case of SBR/filler composite. The beginning degradation temperature of these composites follows the order of metakaolinite /SBR < Al_2O_3/SBR < Kaolin / SBR < Zeolite Na-A /SBR < zeolite Na-A/Al_2O_3/SBR (Table 10).

Moreover, during the temperature range between 500 °C and 600 °C, the mass residue of metakaolinite /SBR composites is always the lowest at any given temperature, while that of Zeolite Na-A /SBR is always the highest (Fig. 6). These results suggest that introducing Zeolite Na-A could improve the thermal stability of SBR composites.

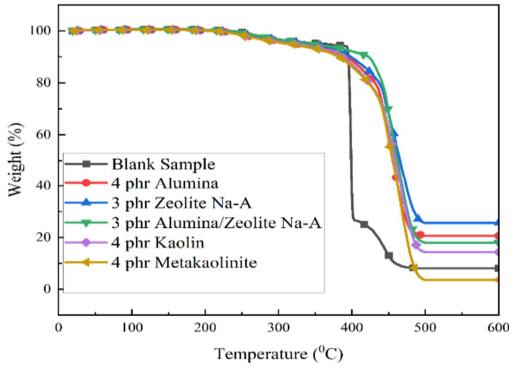

Figure 6: TGA curves of (a) weight (%) for tested samples

Table 10: Temperature degradation statistics for SBR loaded with various fillers (SBR/filler composites)

Samples	T_i (^{0}C)	$T_{25\%}$ (^{0}C)	$T_{50\%}$ (^{0}C)	$T_{75\%}$ (^{0}C)	Residual weights (%)
Unfilled sample	209.39	397	399	417	7.929
4 phr Al_2O_3	196.67	439	456	476	20.628
3 phr Zeolite Na-A	206.23	444	466	499	25.484
3 phr zeolite Na-A/Al_2O_3	207.73	446	462	480	17.878
4 phr Kaolin	201.86	436	459	478	13.973
4 phr Metakaolinite	181.45	434	456	471	3.413

3.5. *Scanning electron microscopy (SEM)*

SEM Fig. 7 was used to analyze the morphologies of tensile fracture surfaces to confirm the various filler-rubber interfacial interactions in SBR composites. Fig. 7 (a) illustrates that pure SBR appears to have a reasonably smooth surface. In contrast, composites have a much more convoluted and rougher morphology with filler, indicating that much energy was absorbed during tensile, and the tensile properties are significantly enhanced. Compared to the fracture surfaces of samples with the same filler contents, the cured sample containing zeolite Na-A/Al_2O_3 produced a high tear cracked surface of the rubber compounds, as shown in Fig. 7 (d).

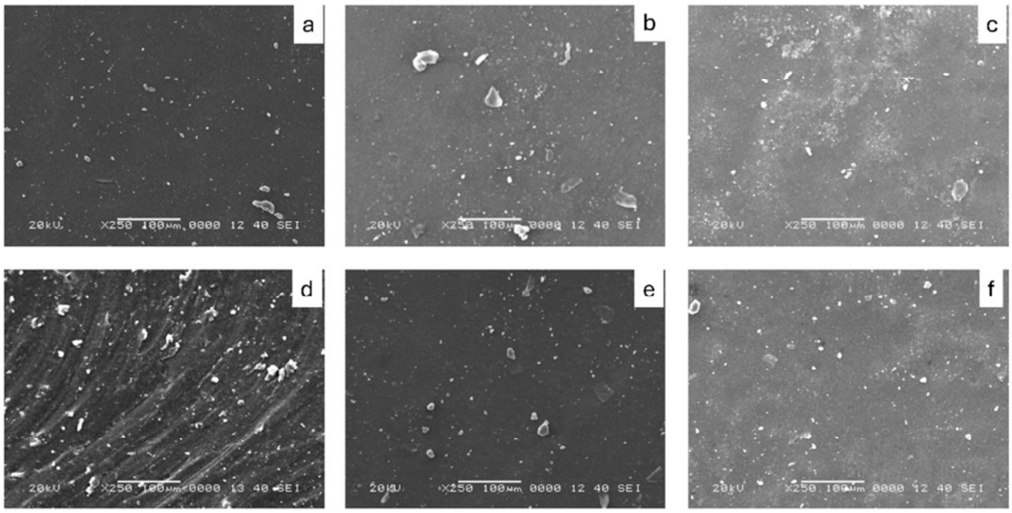

Figure 7: SEM images of SBR rubber composites (a) control sample, (b) 4 phr of treated Al_2O_3, (c) 3 phr of treated Zeolite Na-A, (d) 3 phr of treated zeolite Na-A/Al_2O_3, (e) 4 phr of treated Kaolin, and (f) 4 phr of treated Metakaolinite

4. Conclusion

Thermal stability is an essential feature of any elastomer for its potential applications. Thermal aging of SBR composites reduces elongation and tensile strength at break. This can be explained by the rapid oxidative disintegration that produced a substantial drop. SBR vulcanizates' mechanical properties deteriorate with longer age durations. This has to do with the formation of a high-oxidation process that results in chain scission. Synthetic zeolite Na-A/Al_2O_3 /SBR composite outperformed other fillers for anti-aging effects.

5. Declaration of competing interest

The authors declare that they have no known competing financial interests or personal relationships that could have appeared to influence the work reported in this paper.

6. Acknowledgments

The authors thank the Polymers and Pigments Department, National Research Centre, Cairo, Egypt. Also, the authors thank the Mechanical Engineering Department, Benha Faculty of Engineering, Benha University, Benha, Egypt.

7. References

[1] S. Rasouli, A. Zabihi, M. Fasihi, G.B.P. Kharat, A Comprehensive Study on the Effect of Highly Thermally Conductive Fillers on Improving the Properties of SBR/BR-Filled Nano-Silicon Nitride, ACS Omega. 8 (2023) 32701–32711. https://doi.org/10.1021/acsomega.3c03548.

[2] J. Li, D. Zheng, Z. Yao, S. Wang, R. Xu, S. Deng, B. Chen, J. Wang, Formation Mechanism of Monocyclic Aromatic Hydrocarbons during Pyrolysis of Styrene Butadiene Rubber in Waste Passenger Car Tires, ACS Omega. 7 (2022) 42890–42900. https://doi.org/10.1021/acsomega.2c04994.

[3] A. Nassar, D.S. Mahmoud, W.S. Mohamed, A.M. Moustafa, S.H. El-Sabbagh, Investigation of the structure, magnetic, rheological and mechanical properties of EPDM rubber/Cu-Al-Zn alloy composites, Egypt. J. Chem. 64 (2021) 7277–7291. https://doi.org/10.21608/EJCHEM.2021.79716.3918.

[4] P. Sae-Oui, K. Suchiva, C. Sirisinha, W. Intiya, P. Yodjun, U. Thepsuwan, Effects of Blend Ratio and SBR Type on Properties of Carbon Black-Filled and Silica-Filled SBR/BR Tire Tread Compounds, Adv. Mater. Sci. Eng. 2017 (2017). https://doi.org/10.1155/2017/2476101.

[5] L. Wang, Z. Luo, L. Yang, J. Zhong, Y. Xu, Synergistic Effect of Styrene and Carbon Black on the Fatigue Properties of Styrene-Butadiene Rubber Composites, ACS Omega. 9 (2024) 2000–2011. https://doi.org/10.1021/acsomega.3c09872.

[6] A.A. Abdelsalam, S.H. El-Sabbagh, W.S. Mohamed, J. Li, L. Wang, H. Ismail, A. Abdelmoneim, M.A. Khozami, Effect of compatibilisers on the cure characteristics and mechanical properties of ternary rubber blend composites, Pigment Resin Technol. (2022). https://doi.org/10.1108/PRT-10-2021-0123.

[7] E.E. Ateia, D.E. El-Nashar, H.H. Hassan, A.K. Abd El-Aziz, A comparative study of the cure characteristics, mechanical properties and abrasion resistance of silica and carbon black filled NBR/SBR blends, Egypt. J. Chem. 60 (2017) 769–777. https://doi.org/10.21608/ejchem.2017.828.1033.

[8] S. He, F. Bai, S. Liu, H. Ma, J. Hu, L. Chen, J. Lin, G. Wei, X. Du, Aging properties of styrene-butadiene rubber nanocomposites filled with carbon black and rectorite, Polym. Test. 64 (2017) 92–100. https://doi.org/10.1016/j.polymertesting.2017.09.017.

[9] A.A. Abdelsalam, S.H. El-Sabbagh, W.S. Mohamed, M.A. Khozami, Studies on swelling behavior, mechanical and thermal properties of ternary rubber blend composites in the presence of compatibilizers, Pigment Resin Technol. (2022). https://doi.org/10.1108/PRT-02-2022-0020.

[10] J. Liu, X. Li, L. Xu, P. Zhang, Investigation of aging behavior and mechanism of nitrile-butadiene rubber (NBR) in the accelerated thermal aging environment, Polym. Test. 54 (2016) 59–66. https://doi.org/10.1016/j.polymertesting.2016.06.010.

[11] A.A. Abdelsalam, A.A. Ward, G. Abdel-Naeem, W.S. Mohamed, S.H. El-Sabbagh, Effect of Alumina Modified by Silane on the Mechanical, Swelling and Dielectric Properties of Al2O3/EPDM/SBR Blend Composites, Silicon. (2023). https://doi.org/10.1007/s12633-023-02290-0.

[12] E. V. Bystritskaya, A.L. Pomerantsev, O.Y. Rodionova, Evolutionary design of experiment for accelerated aging tests, Polym. Test. 19 (2000) 221–229. https://doi.org/10.1016/S0142-9418(98)00077-4.

[13] G.R. Hamed, J. Zhao, Tensile behavior after oxidative aging of gum and black-filled

vulcanizates of SBR and NR, Rubber Chem. Technol. 72 (1999) 721–730. https://doi.org/10.5254/1.3538829.

[14] T. Ha-Anh, T. Vu-Khanh, Prediction of mechanical properties of polychloroprene during thermo-oxidative aging, Polym. Test. 24 (2005) 775–780. https://doi.org/10.1016/j.polymertesting.2005.03.016.

[15] A. Mostafa, A. Abouel-Kasem, M.R. Bayoumi, M.G. El-Sebaie, The influence of CB loading on thermal aging resistance of SBR and NBR rubber compounds under different aging temperature, Mater. Des. 30 (2009) 791–795. https://doi.org/10.1016/j.matdes.2008.05.065.

[16] H.A. Raslan, E.S. Fathy, S.E. Abdel Aal, Thermal aging and automotive oil effects on the performance of electron beam irradiated styrene butadiene rubber/waste and microwave devulcanized rubber blends, Prog. Rubber, Plast. Recycl. Technol. 39 (2023) 40–63. https://doi.org/10.1177/14777606221136148.

[17] N. Rezig, T. Bellahcene, M. Aberkane, M. Nait Abdelaziz, Thermo-oxidative ageing of a SBR rubber: effects on mechanical and chemical properties, J. Polym. Res. 27 (2020) 1–13. https://doi.org/10.1007/s10965-020-02330-y.

[18] S. El-Sabbagh, A. Yehia, Detection of Crosslink Density by Different Methods for Natural Rubber Blended with SBR and NBR, Egypt J. Solids. 30 (2007) 157–173. https://doi.org/10.1038/nchem246.

[19] A. A Abdelsalam, M. Demiral, M.M. Selim, S.H. El-Sabbagh, Effect of filler surface treatment on the physico-mechanical properties of filler/styrene-butadiene rubber nanocomposites, J. Thermoplast. Compos. Mater. (2024). https://doi.org/10.1177/08927057241244708.

[20] ASTM D412-06, Standard Test Methods for Vulcanized Rubber and Thermoplastic Elastomers–Tension, ASTM Int. West Conshohocken, PA. (2006) 1–14. https://doi.org/10.1520/D0412-16.

[21] ASTM D573-04, Standard Test Method for Rubber—Deterioration in an Air Oven, ASTM Int. West Conshohocken, PA. (2019) 1–6. https://doi.org/10.1520/D0573-04R19.

[22] S.T. Method, Standard Test Method for Rubber Property — Effect of Liquids 1, Change. i (2012) 1–15. https://doi.org/10.1520/D0471-15.

[23] O. Lorenz, C.R. Parks, The crosslinking efficiency of some vulcanizing agents in natural rubber, J. Polym. Sci. 50 (1961) 299–312. https://doi.org/10.1002/pol.1961.1205015404.

[24] J.I. Cunneen, R.M. Russell, Occurrence and Prevention of Changes in the Chemical Structure of Natural Rubber Tire Tread Vulcanizates during Service, Rubber Chem. Technol. 43 (1970) 1215–1224. https://doi.org/10.5254/1.3547319.

[25] M. Mooney, A theory of large elastic deformation, J. Appl. Phys. 11 (1940) 582–592. https://doi.org/10.1063/1.1712836.

[26] M. Gruendken, D. Koda, J. Dryzek, A. Blume, Low molecular weight 'liquid' polymer extended compounds, impact on free volume and crosslink density studied by positron lifetime spectroscopy and stress-strain analysis according to Mooney-Rivlin, Polym. Test. 100 (2021) 107239. https://doi.org/10.1016/j.polymertesting.2021.107239.

[27] N. Sombatsompop, Practical Use of the Mooney-Rivlin Equation for Determination of Degree of Crosslinking of Swollen Nr Vulcanisates, ScienceAsia. 24 (1998) 199–204.

[28] S. Samaržija-Jovanović, V. Jovanović, G. Marković, S. Konstantinović, M. Marinović-Cincović, Nanocomposites based on silica-reinforced ethylene-propylene-diene-monomer/ acrylonitrile-butadiene rubber blends, Compos. Part B Eng. 42 (2011) 1244–1250. https://doi.org/10.1016/j.compositesb.2011.02.008.

[29] N. Ning, Q. Ma, Y. Zhang, L. Zhang, H. Wu, M. Tian, Enhanced thermo-oxidative aging resistance of EPDM at high temperature by using synergistic antioxidants, Polym. Degrad. Stab. 102 (2014) 1–8. https://doi.org/10.1016/j.polymdegradstab.2014.01.037.

[30] G.-Z.Z. Ji-Fang Fu, Li-Ya Chen, Hui Yang, Qing-Dong Zhong, Li-Yi Shi, Wei Deng, Xing Dong, Yi Chen, Mechanical Properties, Chemical and Aging Resistance of Natural Rubber Filled with Nano-Al2O3, Polym. Compos. 33 (2012) 404–411. https://doi.org/https://doi.org/10.1002/pc.22162.

[31] B.T. Poh, M. JALALUDDIN, Tensile,tearand swelling properties of ENR 50/SBR blend, Int. J. Polym. Mater. Polym. Biomater. 46 (2000) 663–672. https://doi.org/10.1080/00914030008033904.

[32] D.E. El-Nashar, G. Turky, Effect of mixing conditions and chemical cross-linking agents on the physicomechanical and electrical properties of NR/NBR blends, Polym. - Plast. Technol. Eng. 42 (2003) 269–284. https://doi.org/10.1081/PPT-120017929.

[33] K.S.A. Zaher, S.H. El-sabbagh, F.M. Abdelrazek, G.A.M. Nawwar, Utility of Zinc (Lignin / Silica / Fatty Acids) Complex Driven From Rice Straw as Antioxidant and Activator in Rubber Composites, (2019). https://doi.org/10.1002/pen.25029.

[34] G.M. Nasr, A.S. Gomaa, The influence of physical ageing on the electrical and swelling behaviour of ternary rubber vulcanizates, Polym. Degrad. Stab. 50 (1995) 249–259. https://doi.org/10.1016/0141-3910(95)00168-9.

[35] A.P. De Carvalho, H.F. Dos Santos, G.D. Ribeiro, C.T. Hiranobe, D. Goveia, E.M. Gennaro, L.L. Paim, R.J. Dos Santos, Sustainable Composites: Analysis of Filler–Rubber Interaction in Natural Rubber–Styrene–Butadiene Rubber/Polyurethane Composites Using the Lorenz–Park Method and Scanning Electron Microscopy, Polymers (Basel). 16 (2024). https://doi.org/10.3390/polym16040471.

[36] A.A. Abdelsalam, S. Araby, M.A. Hassan, A.A. El-Moneim, Constitutive modelling of elastomer/graphene platelet nanocomposites, IOP Conf. Ser. Mater. Sci. Eng. 244 (2017) 1–8. https://doi.org/10.1088/1757-899X/244/1/012016.

.